Gene fusions *AHRR-NCOA2*, *NCOA2-ETV4*, *ETV4-AHRR*, *P4HA2-TBCK*, and *TBCK-P4HA2* resulting from the translocations t(5;8;17)(p15;q13;q21) and t(4;5)(q24;q31) in a soft tissue angiofibroma

IOANNIS PANAGOPOULOS[1,2], LUDMILA GORUNOVA[1,2], TROND VISET[3] and SVERRE HEIM[1,2,4]

[1]Section for Cancer Cytogenetics, Institute for Cancer Genetics and Informatics, The Norwegian Radium Hospital, Oslo University Hospital, Oslo; [2]Centre for Cancer Biomedicine, Faculty of Medicine, University of Oslo, Oslo; [3]Department of Pathology and Medical Genetics, St. Olavs Hospital, Trondheim University Hospital, Trondheim; [4]Faculty of Medicine, University of Oslo, Oslo, Norway

Received March 25, 2016; Accepted July 18, 2016

DOI: 10.3892/or.2016.5096

Abstract. We present an angiofibroma of soft tissue with the karyotype 46,XY,t(4;5)(q24;q31),t(5;8;17)(p15;q13;q21)[8]/46,XY,t(1;14)(p31;q32)[2]/46,XY[3]. RNA-sequencing showed that the t(4;5)(q24;q31) resulted in recombination of the genes *TBCK* on 4q24 and *P4HA2* on 5q31.1 with generation of an in-frame *TBCK-P4HA2* and the reciprocal but out-of-frame *P4HA2-TBCK* fusion transcripts. The putative TBCK-P4HA2 protein would contain the kinase, the rhodanese-like domain, and the Tre-2/Bub2/Cdc16 (TBC) domains of TBCK together with the P4HA2 protein which is a component of the prolyl 4-hydroxylase. The t(5;8;17)(p15;q13;q21) three-way chromosomal translocation targeted *AHRR* (on 5p15), *NCOA2* (on 8q13), and *ETV4* (on 17q21) generating the in-frame fusions *AHRR-NCOA2* and *NCOA2-ETV4* as well as an out-of-frame *ETV4-AHRR* transcript. In the AHRR-NCOA2 protein, the C-terminal part of AHRR is replaced by the C-terminal part of NCOA2 which contains two activation domains. The NCOA2-ETV4 protein would contain the helix-loop-helix, PAS_9 and PAS_11, CITED domains, the SRC-1 domain of NCOA2 and the ETS DNA-binding domain of ETV4. No fusion gene corresponding to t(1;14)(p31;q32) was found. Our findings indicate that, in spite of the recurrence of *AHRR-NCOA2* in angiofibroma of soft tissue, additional genetic events (or fusion genes) might be required for the development of this tumor.

Correspondence to: Dr Ioannis Panagopoulos, Section for Cancer Cytogenetics, Institute for Cancer Genetics and Informatics, The Norwegian Radium Hospital, Oslo University Hospital, Montebello, P.O. Box 49534 Nydalen, NO-0424 Oslo, Norway
E-mail: ioannis.panagopoulos@rr-research.no

Key words: angiofibroma of soft tissue, cytogenetics, fusion genes, *AHRR-NCOA2*, *NCOA2-ETV4*, *TBCK-P4HA2*, RNA-sequencing

Introduction

Angiofibroma of soft tissue is a recently described benign fibrovascular tumor of unknown cellular origin (1). It arises most commonly in the extremities of middle-aged adults but displays a broad anatomic and age distribution. Microscopically, it is characterized by bland, uniform, probably fibroblastic spindle cell set in an abundant fibromyxoid stroma, with a prominent and highly characteristic vascular pattern composed of innumerable branching, thin-walled blood vessels (1). Cytogenetic knowledge about angiofibroma of soft tissue is based on the analysis of six such tumors of which four showed a balanced t(5;8)(p15;q12) translocation and a fifth tumor showed a three-way t(5;8;8)(p15;q13;p11) (1). Molecular analysis of four tumors carrying the t(5;8)(p15;q12) showed in-frame *AHRR-NCOA2* and *NCOA2-AHHR* fusion transcripts in all of them (2). A *GTF2I-NCOA2* fusion gene was detected in a fifth tumor carrying a t(7;8;14)(q11;q13;q31) as the sole chromosome change (3). To the best of our knowledge, the above-mentioned tumors are the only angiofibromas of soft tissue which have been investigated both cytogenetically and molecularly for fusion genes. An additional angiofibroma of soft tissue with t(5;8)(p15;q12) was also reported but without molecular analysis (4). In three other studies, fluorescence *in situ* hybridization (FISH) was performed with probes for *NCOA2* showing rearrangements of the *NCOA2*; however, no further investigation of fusion genes was performed (5-7).

We report here an angiofibroma of soft tissue which had the chromosome translocations t(4;5)(q24;q31) and t(5;8;17)(p15;q13;q21) and identified the fusion genes generated by the two translocations. Our data show that, in addition to the reported *AHRR-NCOA2*, the tumor carried also other fusion genes resulting from the chromosomal aberrations that might have contributed to tumorigenesis as well.

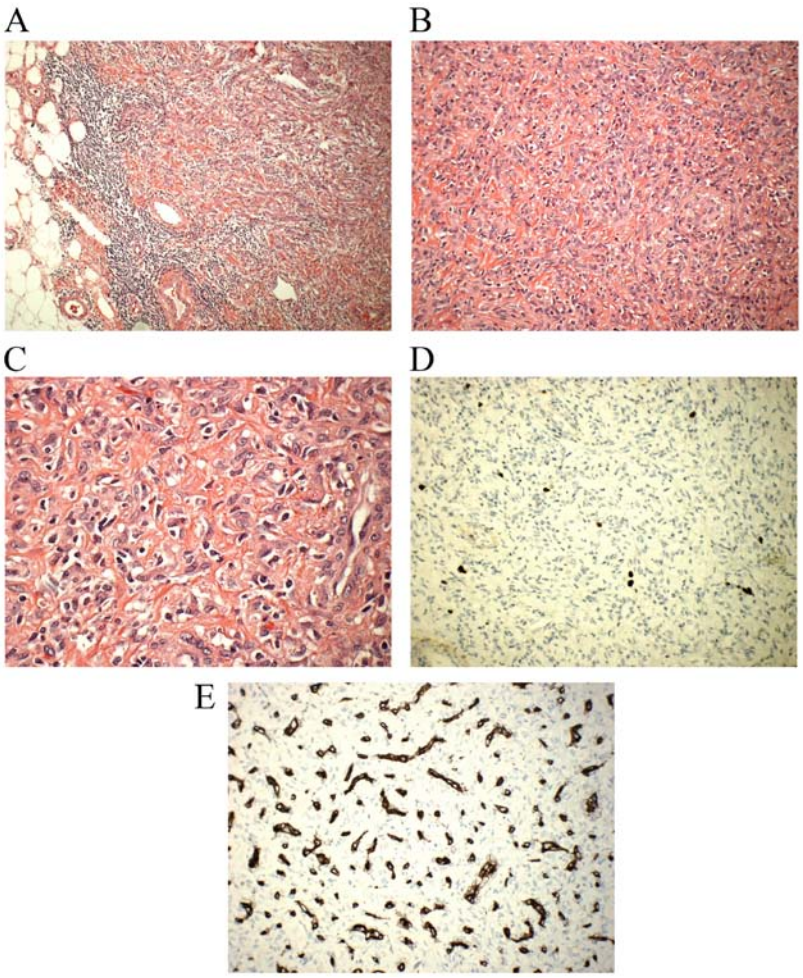

Figure 1. Microscopic examination of the angiofibroma of soft tissue. (A) H&E-100x. (B) H&E-200x. (C) H&E-400x. (D) Immunoexpression of MIB1-200x. (E) Immunoexpression of CD34-200x.

Materials and methods

Ethics statement. The study was approved by the regional Ethics Committee (Regional komité for medisinsk forskningsetikk Sør-Øst, Norge; http://helseforskning.etikkom.no), and written informed consent was obtained from the patient to publication of the case details. The Ethics Committee's approval included a review of the consent procedure. All patient information has been de-identified.

Case history. The patient was a 45-year-old male in whom MRI of the abdomen and pelvis showed a 53-mm tumor in the right inguinal region partially surrounding large vessels. The patient had been aware of the lesion for several years. Surgery was performed with removal of the entire tumor including part of the right deep femoral artery with immediate reconstruction of the vessel. The postoperative period was eventless and to date there is no sign of tumor relapse.

The specimen (58x45x45 mm) showed an encapsuled, well-circumscribed tumor with a homogenous gray/white cut surface. There were no signs of necrosis or bleeding. Routine microscopy showed a tumorous proliferation of small, spindled cells without atypia or mitotic activity (Fig. 1A-C). There were a lot of small, thin-walled blood vessels in the background (Fig. 1A-C). Immunohistochemical examination showed low proliferative activity (MIB1/Ki67 <5%) (Fig. 1D) and the vessels highlighted by the endothelial marker CD34 (Fig. 1E). The clinical setting as well as histopathological features fit well with a diagnosis of angiofibroma of soft tissue (1).

G-banding and karyotyping. Fresh tissue from the tumor was processed for cytogenetic analysis as part of our diagnostic routine. The sample was disaggregated mechanically and enzymatically with collagenase II (Worthington Biochemical Corp., Freehold, NJ, USA). The resulting cells were cultured and harvested using standard techniques. Chromosome preparations were G-banded with Wright stain and examined. The karyotype was written according to the International System for Human Cytogenetic Nomenclature (ISCN) 2013 guidelines (8).

High-throughput paired-end RNA-sequencing. Total RNA was extracted using miRNeasy Mini Kit according to the manufacturer's instructions (Qiagen, Hilden, Germany). Tumor tissue was disrupted and homogenized in QIAzol Lysis Reagent (Qiagen) using a 5-mm stainless steel bead and TissueLyser II (Qiagen). Subsequently, total RNA was purified using QIAcube (Qiagen). The RNA quality was evaluated using the Experion Automated Electrophoresis System (Bio-Rad

Table I. Primers used for PCR amplification and Sanger sequencing analyses.

Name	Sequence (5'→3')	Position	Reference sequence	Gene
TBCK-2908R1	TGGCGTGGATATGAAGAACTGTGC	2931-2908	NM_033115.4	*TBCK*
TBCK-2558F1	CCTGGTGGTTGACATCCGGAATAG	2558-2581	NM_033115.4	*TBCK*
P4HA2-785R1	AGCCAGGTAGCCCTCAGCATCAG	807-785	NM_004199.2	*P4HA2*
P4HA2-33F1	CCGCGGGAGGTTCTGGAAAC	33-52	NM_001142598.1	*P4HA2*
NCOA2-intr14-R1	CACCATGTCGAGACTGCTGGCTC	71106777-71106799	NC_018919.2	*NCOA2*
NCOA2-3364R1	TCACTCGGAGACTCAGCTGCAGG	3386-3364	NM_006540.2	*NCOA2*
NCOA2-2858F1	CTGGACCTTTCCCACCAATCAGAA	2858-2881	NM_006540.2	*NCOA2*
ETV4-1496R1	GGGGCTCTCATCCAAGTGGGAC	1517-1496	NM_001986.2	*ETV4*
ETV4-863F1	TGGGGTCAATGGGCACAGGTAC	863-884	NM_001986.2	*ETV4*
AHRR-1932R1	TGCAGGGTGGAAAGGGGTCAG	1952-1932	NM_020731.4	*AHRR*
AHRR-1503F1	AGCAGACCCATGCGGGATGTC	1503-1523	NM_020731.4	*AHRR*
AHRR-1425F1	TGTGTCCAGGGCACTTTCAGGAA	1425-1447	NM_020731.4	*AHRR*
EGFL7-353F1	ACCCCAAAGCCACATCTGTAGCC	353-375	NM_016215.4	*EGFL7*
MCF2L-3271R1	CGCCACGACCGTGTATTTACCTG	3293-3271	NM_024979.4	*MCF2L*
CYP1B1-132F1	TCAACGCTGTGAGGAAACCTCGA	132-154	NM_000104.3	*CYP1B1*
CLU-1164R1	GACCTGGAGGGATTCGTCGAGC	1185-1164	NM_001831.3	*CLU*

Laboratories, Oslo, Norway). The RNA quality indicator (RQI) was 8.5. Total RNA (3 μg) was sent for high-throughput paired-end RNA-sequencing at the Norwegian Sequencing Centre, Ullevål Hospital (http://www.sequencing.uio.no/). Detailed information about the high-throughput paired-end RNA-sequencing was given elsewhere (9). The software FusionCatcher (10) (https://github.com/ndaniel/fusioncatcher) was used for the discovery of fusion transcripts.

Molecular genetic analyses. The primers used for PCR amplification and sequencing are listed in Table I. The primer combinations, target fusion transcripts, and results of PCR amplifications are shown in Table II. cDNA was synthesized from 2 μg of total RNA in a 20-μl reaction volume using iScript Advanced cDNA Synthesis Kit for RT-qPCR according to the manufacturer's instructions (Bio-Rad Laboratories). cDNA was diluted to 100 μl and 2 μl were used as template in subsequent PCR assays. The 25-μl PCR volumes contained 12.5 μl of Premix Taq (Takara Bio Europe SAS, Saint-Germain-en-Laye, France), 1 μl of diluted cDNA, and 0.4 μM of each of the forward and reverse primers (Table II). The quality of the cDNA synthesis was examined by amplification of a cDNA fragment of the *TBCK* gene using the primers TBCK-2558F1 and TBCK-2908R1. The PCRs were run on a C1000 Thermal cycler (Bio-Rad Laboratories) with the following cycling for the amplifications: an initial denaturation at 94˚C for 30 sec, 35 cycles of 7 sec at 98˚C, 7 sec at 60˚C, 1 min at 72˚C, and a final extension for 5 min at 72˚C.

The PCR products were analyzed on a QIAxcel Advanced System according to the manufacturer's instructions (Qiagen). The remaining PCR products were purified using the QIAquick PCR Purification Kit or the QIAquick Gel Extraction Kit (both from Qiagen) and direct sequenced using the dideoxy procedure with the ABI Prism BigDye Terminator v1.1 Cycle Sequencing Kit (Applied Biosystems, Foster City, CA, USA) on the Applied Biosystems 3500 Genetic Analyzer sequencing system. The BLAST software (http://www.ncbi.nlm.nih.gov/BLAST/) was used for computer analysis of the sequence data.

Table II. Primer combinations, target fusion transcripts and results of PCR amplification.

Primer combination	Target fusion transcripts	Results
P4HA2-33F1/TBCK-2908R1	*P4HA2-TBCK*	Positive
TBCK-2558F1/P4HA2-785R1	*TBCK-P4HA2*	Positive
AHRR-1503F1/NCOA2-intr14-R1	*AHRR-NCOA2*	Positive
AHRR-1425F1/NCOA2-3364R1	*AHRR-NCOA2*	Positive
ETV4-863F1/AHRR-1932R1	*ETV4-AHRR*	Positive
NCOA2-2858F1/ETV4-1496R1	*NCOA2-ETV4*	Positive
EGFL7-353F1/MCF2L-3271R1	*EGFL7-MCF2L*	Negative
CYP1B1-132F1/CLU-1164R1	*CYP1B1-CLU*	Negative

Results

Cytogenetic analysis. The G-banding analysis showed that the tumor had two cytogenetically unrelated clones. The first clone, found in eight metaphases, had the t(4;5)(q24;q31) and t(5;8;17)(p15;q13;q21) chromosome aberrations (Fig. 2A). The second, found in two metaphases, had the t(1;14)(p31;q32) abnormality (Fig. 2B). This yielded the following karyotype: 46,XY,t(4;5)(q24;q31),t(5;8;17)(p15;q13;q21)[8]/46,XY,t(1;14)(p31;q32)[2]/46,XY[3].

High-throughput paired-end RNA-sequencing analysis. Using the FusionCatcher software with the FASTQ files obtained

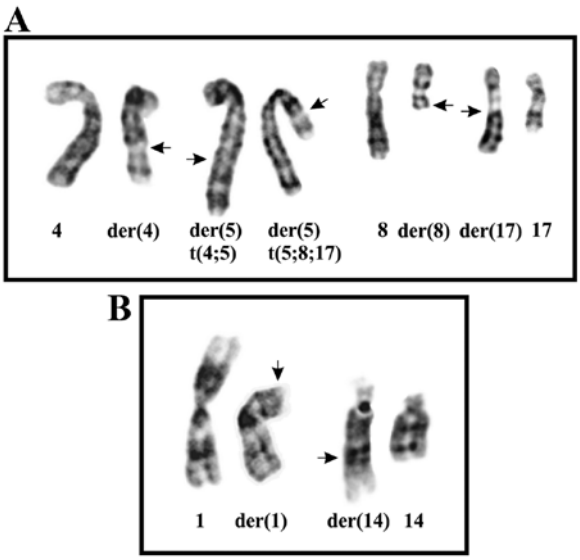

Figure 2. Cytogenetic analysis of the angiofibroma of soft tissue. (A) Partial karyotype showing from left to right the chromosomes 4, der(4)t(4;5)(q24;q31), der(5)t(4;5)(q24;q31), der(5)t(5;8;17)(p15;q13;q21), 8, der(8)t(5;8;17)(p15;q13;q21), der(17)t(5;8;17)(p15;q13;q21), and 17. (B) Partial karyotype showing the der(1)t(1;14)(p31;q32) and der(14)t(1;14)(p31;q32) together with the corresponding normal chromosome homologs. Breakpoint positions are indicated by arrows.

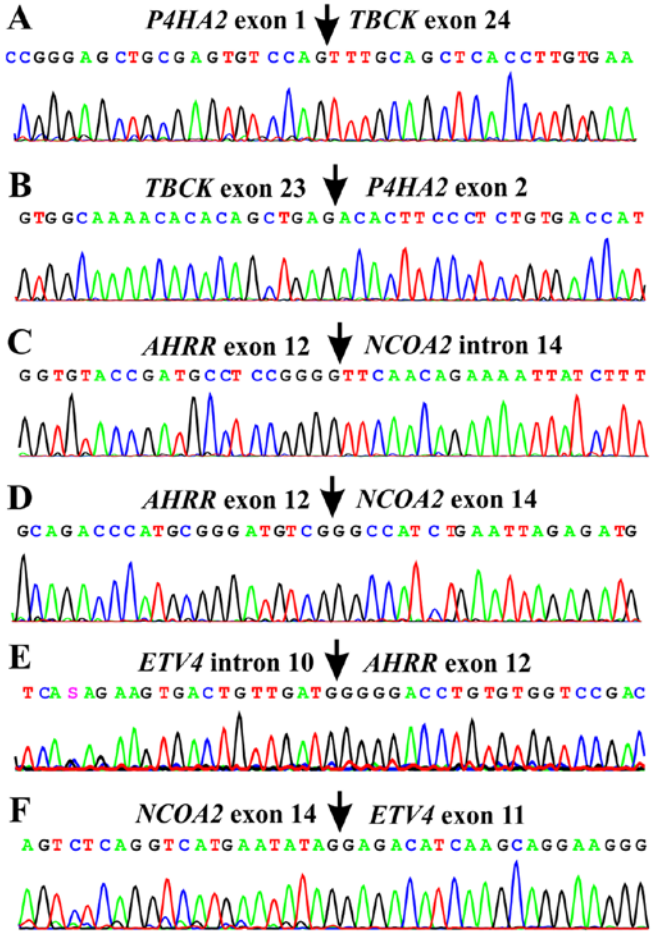

Figure 3. Partial sequence chromatogram of the amplified cDNA fragment showing the junction points of the fusion transcripts. (A) *P4HA2-TBCK*, (B) *TBCK-P4HA2*, (C) exon 12 of *AHRR* with sequence of intron 14 of *NCOA2*, (D) exon 12 of *AHRR* with exon 14 of *NCOA2*, (E) *ETV4-AHRR*, and (F) *NCOA2-ETV4*.

from the Norwegian Sequencing Centre, Ullevål Hospital (http://www.sequencing.uio.no/), 39 potential fusions were found: 28 fusions were described as readthrough short-distance fusions and 5 as pseudogenes (Table III). Among the other fusions, the program detected the *P4HA2-TBCK* and the reciprocal *TBCK-P4HA2*. According to the UCSC Genome Browser on Human, Feb. 2009, (GRCh37/hg19) assembly (http://genome-euro.ucsc.edu/cgi-bin/hgGateway), *P4HA2* maps on chromosome subband 5q31.1 and *TBCK* on band 4q24. Thus, the two fusions *P4HA2-TBCK* and the reciprocal *TBCK-P4HA2* most probably were the result of the balanced chromosome translocation t(4;5)(q24;q31). FusionCatcher also detected *AHRR-NCOA2* and *ETV4-AHRR* which correspond to the three-way t(5;8;17)(p15;q13;q21) found in the tumor. The three genes *AHRR*, *NCOA2*, and *ETV4* map to chromosome subbands 5p15.33, 8q13.3, and 17q21.31, respectively (https://genome.ucsc.edu/). In the three-way t(5;8;17), the moving of 5p15 to 8q13 generated the *AHRR-NCOA2* fusion whereas the translocation of 17q21 to 5p15 generated the *ETV4-AHRR*. We assume that the moving of 8q13 to 17q21 would have generated an *NCOA2-ETV4* fusion but no such fusion was, for unknown reasons, detected by FusionCatcher. The fusion transcrips *EGFL7-MCF2L* and a *CYP1B1-CLU* were also detected by the analysis with FusionCatcher, in all likelihood generated by t(9;13)(q34;q34) and t(2;8)(p22.2;p21.1), respectively. No fusion gene corresponding to the cytogenetically detected t(1;14)(p31;q32) was found.

We decided to investigate with molecular methods the described fusion transcripts. No other fusions were examined.

Molecular genetic confirmation of fusions. PCR with the primers TBCK-2558F1 and TBCK-2908R1 amplified a cDNA of the *TBCK* gene indicating that the synthesized cDNA was of good quality.

RT-PCR using cDNA from the tumor and subsequent direct Sanger sequencing verified the presence of the *P4HA2-TBCK*, *TBCK-P4HA2*, *AHRR-NCOA2*, *ETV4-AHRR*, and *NCOA2-ETV4* fusion transcripts (Table II and Fig. 3). *TBCK-P4HA2*, *AHRR-NCOA2*, and *NCOA2-ETV4* were in-frame fusions which would code for chimeric proteins. The detected *ETV4-AHRR* fusion, on the other hand, was out-of-frame and would not produce a chimeric protein, nor would the *P4HA2-TBCK* code for any functional protein. No *EGFL7-MCF2L* or *CYP1B1-CLU* fusion transcript was found by RT-PCR amplification (Table II).

Discussion

The examined angiofibroma of soft tissue carried the recurrent *AHRR-NCOA2* fusion transcript but lacked the reciprocal *NCOA2-AHRR*. This finding supports the initial suggestion that *AHRR-NCOA2* is the pathogenetically significant fusion transcript in tumors carrying a t(5;8)(p15;q12) (2,3). While we were examining the current tumor, a report was published describing 13 cases of angiofibroma of soft tissue with an *AHRR-NCOA2* but with only eight of them carrying the reciprocal *NCOA2-AHRR* (11). Current data therefore agree that the *AHRR-NCOA2* fusion gene is recurrent in angiofibroma of

Table III. Fusion transcripts detected using FusionCatcher.

5'-Partner gene	3'-Partner gene	Fusion description	Fusion sequence
PCDP1	*TMEM177*	Readthrough	ATTCTAGAATGAAAGTCACCAGTAG*gaaagggaacatcacagaaaggtga
MIR155HG	*JAM2*	Readthrough	CAAGGAGACGCTCCTGGCACTGCAG*atcataaggcctatgggttttctgc
GOLT1A	*KISS1*	Readthrough	ATGATCTCCATCACCGAATGGCAGA*cctcaaggcacttctaggacctgcc
SHISA9	*U91319.1*	Readthrough	AAGTACGCCTCCTTAAAGGCAGTCG*agctggaacacccttcttctcctgc
VPS45	*PLEKHO1*	Readthrough	GCACCACAGTGCACAACACGAAAAG*ggacctcaggatggaaaccagcagc
P4HA2	***TBCK***		**AACGCCGGGAGCTGCGAGTGTCCAG*tttgcagctcaccttgtgaagatga**
TBCK	***P4HA2***		**GCATGTGGCAAAACACACAGCTGAG*acacttccctctgtgaccatgaaac**
ADCK4	*NUMBL*	Readthrough	TCCAGCCTCTCAGTGTGTTGGAGAG*acggggcgggcaccatgaacaagtt
ETV4	***AHRR***		**AAGGTCAGAGAAGTGACTGTTGATG*ggggacctgtgtggtccgacgctgc**
FOSB	*PPM1N*	Readthrough	TCCACCCACCGCCGCCGCCTCCCAG*aaggggcaggatggggctgggaagt
MFSD7	*ATP5I*	Readthrough	GGGGAGGATCCACTTGACTGGACAG*attacctaaaacctcgggcagaaga
DPY19L2	*DPY19L2P2*	Pseudogene	TTCTTCATCTTTGTTAATGACGTGG*ctaattcaaggtagtgcctggtggt
DPY19L2P2	*DPY19L2*	Pseudogene	TTCTTCATCTTTGTTAATGACATGG*ctaattcaaggtagtgcctggtggt
MATR3	*PAIP2*	Readthrough	CCGCGTCCCGCTCGCTGGGAGAGAG*gttaaaaacgacaaccaacatcagc
LINC00893	*LINC00894*	Antisense	AGGAAGCAGGAATGCTGGAGATGAG*acggagttttgctcttgttgcccag
PTPRG	*C3orf14*	Readthrough	GAGGCCTGGAGTATTCACAGACATT*ggcaagcactttaacctttaagcc
SIX3	*AC012354.6*	Readthrough	AGACACCGGCACCTCCATCCTCTCG*acaaggccacctacatcccaagcca
CTBS	*GNG5*	Readthrough	GCGGGCTCCTTATTATAACTATAAA*gtttcccaggcagctgcagacttga
CYP1B1	*CLU*	Readthrough	CGAGTGGGAGTTAAAGCTTCCAGTG*aaggcgacgatgaccggactgtgtg
ZBTB16	*NNMT*	Readthrough	CGGGACCCCCTCAGCCTCATTTCTG*aagggctgaactgatggaaggaatg
KB-1507C5.4	*ATP6V1C1*	Readthrough	TCCATGTCGTAAGTTACACAAGAAG*aatctctcttgatttttgaggaaat
PPP1R21	*STON1*	Readthrough	TGACACACTAAAGATGTCCAGTAAG*gagggagcgctctcccctcctctgg
SUZ12	*SUZ12P*	Pseudogene	GAAACTCCAGAACAAACATCAAAAG*cttgtcagctcatttgcagcttaca
SUZ12P	*SUZ12*	Pseudogene	AAATGACAGTATTTGATAAAAACAG*aggctgcctccattcgaaacatttt
TREM2	*TREML1*	Readthrough	CTGCTCATCTTACTCTTTGTCACAG*catcccttgatctggggtgctgtg
TRIM2	*MND1*	Readthrough	CGACTGGGGAAACAGCAGGATCCAG*tcaaagaaaaaaggactgagtgcag
AC015977.6	*CIB4*	Readthrough	GGTTCTGCCCAGAAGCCAGCTGCAG*gccctgaccttcctgaccagaaatga
AHRR	***NCOA2***		**GCAAGGTGTACCGATGCCTCCGGGG*ttcaacagaaaattatcttttggaa**
CHD4	*NOP2*	Readthrough	GGCACCCGAACCTACCCCACAGCAG*taccatggggcgcaagttggaccct
EGFL7	*MCF2L*		GGGATGACTGATTCTCCTCCGCCAG*gttggagcaaaacgtcccactcact
GPR65	*LINC01146*	Readthrough	AAACACATCACCGGAAGAAATATGG*atgatgcatatcataaattattact
HERC3	*FAM13A-AS1*	Readthrough	AATTCTACATGATTAAAGAATCCAT*ccctttacagaaaacaactgaccaa
KB-1572G7.2	*AP000347.4*	Readthrough	ACACCACTCTTCCTGTTGGCCCAAG*gtcagcccaagactaccccgtcggt
LCAT	*PSMB10*	Readthrough	TGAATAAAGACCTTCCTTTGCTACC*agtacccagtgagcagcacagaggg
LSP1	*TNNT3*	Short-distance	CCGGCTCCCTAGGCGTCCCATCTCG*aaaccacccaccttcaccatgtctg
LTBP2	*NPC2*	Readthrough	GATGCGGCCCACATGGCCTGCGTAG*gttctgtggatggagttataaagga
OSBPL2	*ADRM1*	Readthrough	GGTTGCAAGCTGAGAACATCCAGAG*gaacccaagacagaccaggatgagg
PARL	*MAP6D1*	Readthrough	ATCTTGGGGGAGCTCTTTTTGGAAT*acaggaattccaggcttggactgga
PTPN22	*RSBN1*	Readthrough	AACTCCAGCTCATTTCTGAATTTTG*aaacaccagatgaaaatggtaaaac

soft tissue [(2,3,11), present case] and indicate that this is the pathogenetically crucial outcome of the t(5;8).

Using FISH on formalin-fixed, paraffin-embedded specimens, Sugita *et al* (5) found that 16-36% of the tumor cells showed *NCOA2* rearrangement. A fairly small proportion of *NCOA2* gene rearrangement-positive cells (4-12 split signals per 50 tumor cell nuclei) was recently reported also by Yamada *et al* (11). The split signals were mostly detected in relatively large, spindle-shaped nuclei, indicating that these were the ones belonging to the neoplastic parenchyma (11).

The present tumor had two cytogenetically unrelated clones: one (eight metaphases) with the translocations t(4;5)(q24;q31) and t(5;8;17)(p15;q13;q21) and another (2 cells) with t(1;14)(p31;q32) as the sole chromosome abnormality. Thus, our data not only are in agreement with previous observations that only a fraction of tumor cells carry the *NCOA2* gene rearrangement, but also demonstrate genetic heterogeneity of uncertain pathogenetic significance within the tumor. Although no fusion gene was found corresponding to t(1;14)(p31;q32), this should not lead us to conclude that

the translocation was pathogenetically unimportant. The t(1;14)(p31;q32) chromosome aberration may exert its influence through a position effect causing deregulation of a gene in the proximity of the breakpoints. Alternatively, the current methodology may be unable to detect a fusion gene as has been demonstrated (9).

So far, three types of *AHRR-NCOA2* fusion transcripts have been described: in the first type, exon 9 of *AHRR* is joined with exon 16 of *NCOA2*, the second type shows exon 10 of *AHRR* being joined to exon 14 of *NCOA2*, and in the third type there is an insertion of an intronic sequence from the *NCOA2* gene between exon 9 of *AHRR* and exon 14 of *NCOA2* (2,11). In the present angiofibroma of soft tissue, two novel fusion transcripts were found with different fusion positions from those previously described: a fusion transcript in which nt 1670 (sequence with accession no. NM_020731) from exon 12 of the *AHRR* gene was fused with a sequence from intron 14 of *NCOA2* and a transcript in which nt 1533 (also from exon 12) of *AHRR* was fused to exon 15 of *NCOA2* (sequence with accession no. NM_006540.2). The resulting putative AHRR-NCOA2 protein would be similar to those reported (2) in as much as the C-terminal part of AHRR is replaced by the C-terminal part of NCOA2.

The involvement of *NCOA2* in neoplasia was first reported in acute myeloid leukemia with the cytogenetic inversion inv(8)(p11q13) which resulted in a *KAT6A-NCOA2*, also known as *MOZ-TIF2* fusion gene (12,13). Since then, *NCOA2* has been implicated also in other malignancies. A fusion between *ETV6* (*TEL*) and *NCOA2* was reported in childhood leukemia with the recurrent t(8;12)(q13;p13) (14). A *PAX3-NCOA2* gene was found as a rare variant fusion in alveolar rhabdomyosarcoma; it was brought about by a t(2;8)(q35;q13) translocation (15). A *HEY1-NCOA2* fusion gene was described in mesenchymal chondrosarcomas (16,17). Recently, *SRF-NCOA2*, *TEAD1-NCOA2*, and *VGLL2-NCOA2* fusions were reported in rhabdomyosarcomas (18,19). In all the above-mentioned fusions, *NCOA2* is the 3'-partner gene and all fusion proteins contain the two C-terminal activation domains AD1/CID (activation domain 1/CREB-binding protein interacting domain) and AD2 (2,3,12-19). The transforming activities of *KAT6A-NCOA2* and *PAX3-NCOA2* have been demonstrated experimentally (15,20). In addition, *KAT6A-NCOA2* was shown to induce acute myeloid leukemia in transgenic fish (21). Deguchi *et al* (20) showed that the *KAT6A-NCOA2* interaction with CREBBP through AD1/CID is essential for transformation. Similarly, Sumegi *et al* (15) showed that while deletion of the AD2 portion of PAX3-NCOA2 fusion protein reduced the transforming activity, deletion of the AD1/CID domain fully abrogated the transforming activity of the chimeric protein. Thus, the AD1/CID and AD2 domains of NCOA2 seem to be essential for the transformation ability of the various fusion proteins.

The three-way translocation t(5;8;17)(p15;q13;q21) of the present case not only generated an *AHRR-NCOA2* resulting from the translocation of 5p15 to 8q13, but also two additional fusion genes: an *NCOA2-ETV4*, stemming from the moving of 8q13 to 17q21, and an *ETV4-AHRR*, generated by the moving of 17q21 to 5p15. The detected *ETV4-AHRR* fusion transcript is out-of-frame and so cannot produce a chimeric protein. The *NCOA2-ETV4* fusion transcript is in-frame coding for a chimeric NCOA2-ETV4 protein, the oncogenetic potential of which cannot be ruled out. Based on the NCOA2 and ETV4 proteins with accession nos. NP_006531.1 and NM_001986.2, respectively, the chimeric NCOA2-ETV4 would contain 1,175 amino acids. The NCOA2 N-terminal part of the protein would contain the helix-loop-helix, PAS_9 and PAS_11, the CITED, and the SRC-1 domains. The ETV4 C-terminal part would contain the ETS DNA-binding domain of ETV4 (Fig. 4).

ETV4 was reported to contribute the 3'-part of the oncogenic protein in the subset of Ewing's sarcomas characterized by a t(17;22)(q12;q12) translocation (22,23). The EWSR1-ETV4 protein, in which the N-terminal part of EWSR1 is fused to the ETS DNA-binding domain of ETV4, has an oncogenetic potential similar to that of the EWSR1-FLI1, EWSR1-ERG, EWSR1-FEV, and EWSR1-ETV1 fusion proteins which may also be found in Ewing's sarcoma (24). The *ETV4* gene was also described as the 3'-partner in fusion genes found in prostate carcinoma (25-27). *ETV4* was found to fuse with the *TMPRSS2*, *KLK2*, *CANT1*, and *DDX5* (25-27). All these fusions genes, *TMPRSS2-ETV4*, *KLK2-ETV4*, *CANT1-ETV4*, and *DDX5-ETV4*, contain (like the present *NCOA2-ETV4*) the part of ETV4 coding for the ETS DNA-binding domain.

The chromosome translocation t(4;5)(q24;q31) generated the *P4HA2-TBCK* and *TBCK-P4HA2* fusion transcripts. *P4HA2-TBCK* does not encode any functional protein, whereas *TBCK-P4HA2* encodes a chimeric 1,335-amino acid protein. TBCK-P4HA2 would contain the first 794 out of 830 amino acids of the TBCK protein (accession no. NP_149106.2), 6 amino acids from the untranslated region of exon 2 of P4HA2 (accession no. NM_004199.2), and the entire 535 amino acid-P4HA2 protein (NP_004190.1). The function of this putative chimeric protein is difficult to predict since it would contain both the protein kinase domain, the Rhodanese-like domain, and the Tre-2/Bub2/Cdc16 (TBC) domain of TBCK together with the P4HA2 protein which is a component of the prolyl 4-hydroxylase. The TBCK protein is thought to play a role in actin organization, cell growth, and cell proliferation by regulating the mammalian target of the rapamycin (mTOR) signaling pathway. This protein may also be involved in the transcriptional regulation of the components of the mTOR complex (http://www.ncbi.nlm.nih.gov/gene/93627). Depletion of TBCK significantly inhibits cell proliferation, reduces cell size, and disrupts the organization of actin but not microtubule. Knockdown of TBCK induces a significant decrease in the protein levels of components of mTOR complex (mTORC) and suppresses the activity of mTOR signaling, but not the MAPK or PDK1/Akt pathway (28).

The protein encoded by the *P4HA2* gene is one of several different types of α subunit of the prolyl 4-hydroxylase and provides the major part of the catalytic site of the active enzyme (http://www.ncbi.nlm.nih.gov/gene/8974). In collagen and related proteins, prolyl 4-hydroxylase catalyzes the formation of 4-hydroxyproline that is essential to the proper three-dimensional folding of newly synthesized procollagen chains. In breast cancer, P4HA2 was shown to promote progression and metastasis by regulating collagen deposition (29). In squamous cell carcinoma of the oral cavity, P4HA2 was identified as a metastasis associated protein (30).

In spite of the now repeatedly documented recurrence of *AHRR-NCOA2* in angiofibroma of soft tissue [present

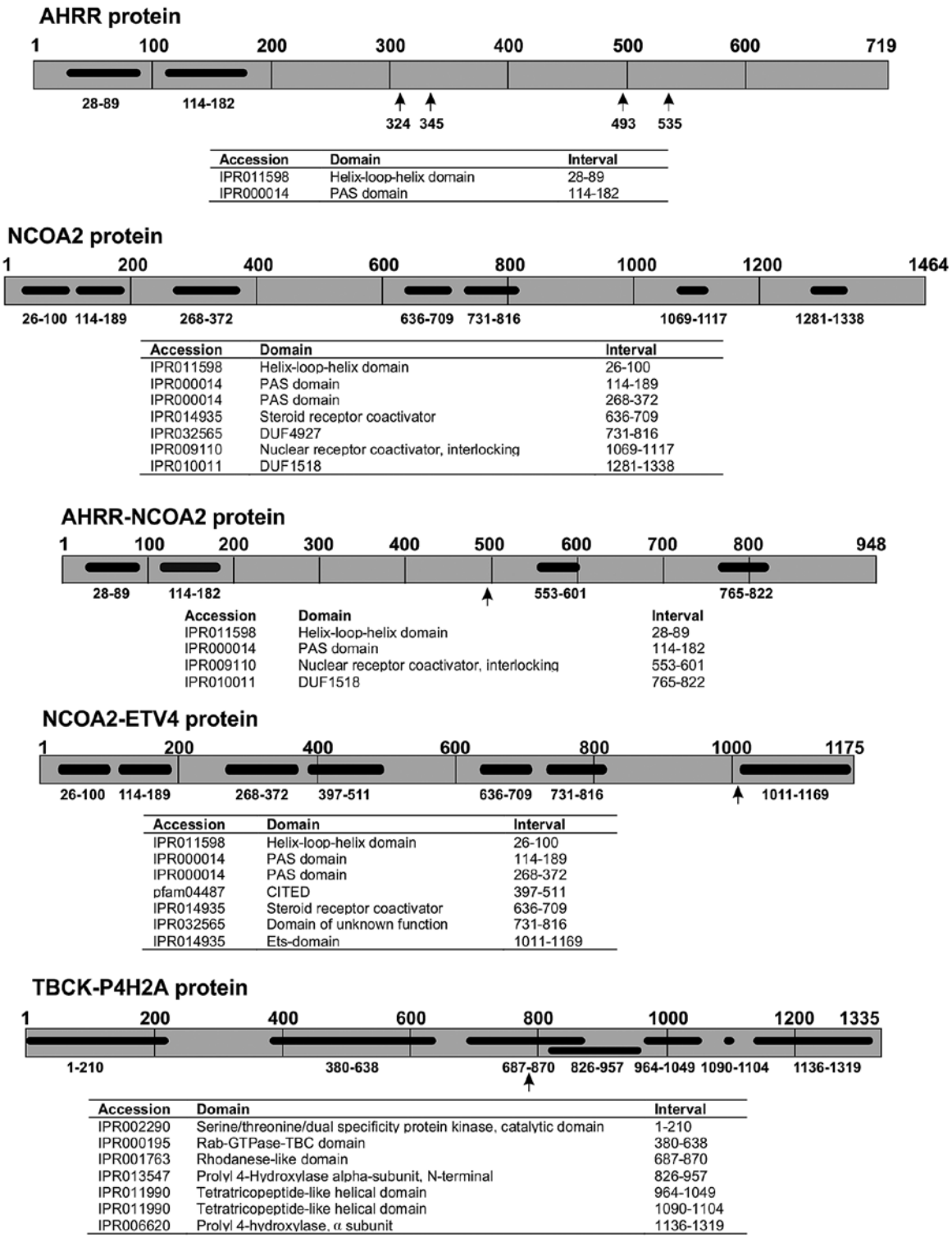

Accession	Domain	Interval
IPR011598	Helix-loop-helix domain	28-89
IPR000014	PAS domain	114-182

Accession	Domain	Interval
IPR011598	Helix-loop-helix domain	26-100
IPR000014	PAS domain	114-189
IPR000014	PAS domain	268-372
IPR014935	Steroid receptor coactivator	636-709
IPR032565	DUF4927	731-816
IPR009110	Nuclear receptor coactivator, interlocking	1069-1117
IPR010011	DUF1518	1281-1338

Accession	Domain	Interval
IPR011598	Helix-loop-helix domain	28-89
IPR000014	PAS domain	114-182
IPR009110	Nuclear receptor coactivator, interlocking	553-601
IPR010011	DUF1518	765-822

Accession	Domain	Interval
IPR011598	Helix-loop-helix domain	26-100
IPR000014	PAS domain	114-189
IPR000014	PAS domain	268-372
pfam04487	CITED	397-511
IPR014935	Steroid receptor coactivator	636-709
IPR032565	Domain of unknown function	731-816
IPR014935	Ets-domain	1011-1169

Accession	Domain	Interval
IPR002290	Serine/threonine/dual specificity protein kinase, catalytic domain	1-210
IPR000195	Rab-GTPase-TBC domain	380-638
IPR001763	Rhodanese-like domain	687-870
IPR013547	Prolyl 4-Hydroxylase alpha-subunit, N-terminal	826-957
IPR011990	Tetratricopeptide-like helical domain	964-1049
IPR011990	Tetratricopeptide-like helical domain	1090-1104
IPR006620	Prolyl 4-hydroxylase, α subunit	1136-1319

Figure 4. Illustration of the proteins AHRR, NCOA2, AHRR-NCOA2, NCOA2-ETV4, and TBCK-P4H2A. The domains, their accession nos., and intervals are also shown. Arrows in the AHRR protein indicate the known fusion points for the published AHRR-NCOA2 proteins. Arrows in the AHRR-NCOA2, NCOA2-ETV4, and TBCK-P4H2A show the fusion points in the present angiofibroma of soft tissue.

case, (2,11)], our findings indicate that also additional genetic events, some of which lead to fusion genes, may be important in tumor development. Worthy of mention is that of the eight hitherto cytogenetically reported tumors, including the present case, three had three-way translocations (1-3). What lies behind this highly unusual feature is unknown. Obviously, more such tumors must be studied cytogenetically and molecularly before all important aspects of their pathogenesis are laid bare.

Acknowledgements

The authors would like to thank Hege Kilen Andersen and Nina Øino for their excellent technical assistance. This study

was supported by grants from the Norwegian Radium Hospital Research Foundation.

References

1. Mariño-Enríquez A and Fletcher CD: Angiofibroma of soft tissue: Clinicopathologic characterization of a distinctive benign fibrovascular neoplasm in a series of 37 cases. Am J Surg Pathol 36: 500-508, 2012.
2. Jin Y, Möller E, Nord KH, Mandahl N, Von Steyern FV, Domanski HA, Mariño-Enríquez A, Magnusson L, Nilsson J, Sciot R, *et al*: Fusion of the AHRR and NCOA2 genes through a recurrent translocation t(5;8)(p15;q13) in soft tissue angiofibroma results in upregulation of aryl hydrocarbon receptor target genes. Genes Chromosomes Cancer 51: 510-520, 2012.
3. Arbajian E, Magnusson L, Mertens F, Domanski HA, Vult von Steyern F and Nord KH: A novel GTF2I/NCOA2 fusion gene emphasizes the role of NCOA2 in soft tissue angiofibroma development. Genes Chromosomes Cancer 52: 330-331, 2013.
4. Schoolmeester JK, Sukov WR, Aubry MC and Folpe AL: Angiofibroma of soft tissue: Core needle biopsy diagnosis, with cytogenetic confirmation. Am J Surg Pathol 36: 1421-1423, 2012.
5. Sugita S, Aoyama T, Kondo K, Keira Y, Ogino J, Nakanishi K, Kaya M, Emori M, Tsukahara T, Nakajima H, *et al*: Diagnostic utility of NCOA2 fluorescence in situ hybridization and Stat6 immunohistochemistry staining for soft tissue angiofibroma and morphologically similar fibrovascular tumors. Hum Pathol 45: 1588-1596, 2014.
6. Fukuda Y, Motoi T, Kato I, Ikegami M, Funata N, Ohtomo R, Horiguchi S, Goto T and Hishima T: Angiofibroma of soft tissue with fibrohistiocytic features and intratumor genetic heterogeneity of NCOA2 gene rearrangement revealed by chromogenic in situ hybridization: A case report. Pathol Int 64: 237-242, 2014.
7. Edgar MA, Lauer SR, Bridge JA and Rizzo M: Soft tissue angiofibroma: Report of 2 cases of a recently described tumor. Hum Pathol 44: 438-441, 2013.
8. Schaffer LG, McGowan-Jordan J and Schmid M (eds): ISCN 2013: An International System for Human Cytogenetic Nomenclature (2013). Recommendations of the International Standing Committee on Human Cytogenetic Nomenclature. 1st edition. S. Karger AG, Basel, 2013.
9. Panagopoulos I, Gorunova L, Bjerkehagen B and Heim S: The 'grep' command but not FusionMap, FusionFinder or ChimeraScan captures the CIC-DUX4 fusion gene from whole transcriptome sequencing data on a small round cell tumor with t(4;19)(q35;q13). PLoS One 9: e99439, 2014.
10. Nicorici D, Satalan M, Edgren H, Kangaspeska S, Murumagi A, Kallioniemi O, Virtanen S and Kilkku O: FusionCatcher - a tool for finding somatic fusion genes in paired-end RNA-sequencing data. bioRxiv 011650; doi: http://dx.doi.org/10.1101/011650.
11. Yamada Y, Yamamoto H, Kohashi K, Ishii T, Iura K, Maekawa A, Bekki H, Otsuka H, Yamashita K, Tanaka H, *et al*: Histological spectrum of angiofibroma of soft tissue: Histological and genetic analysis of 13 cases. Histopathology: Feb 4, 2016 (Epub ahead of print).
12. Carapeti M, Aguiar RC, Goldman JM and Cross NC: A novel fusion between MOZ and the nuclear receptor coactivator TIF2 in acute myeloid leukemia. Blood 91: 3127-3133, 1998.
13. Carapeti M, Aguiar RC, Watmore AE, Goldman JM and Cross NC: Consistent fusion of MOZ and TIF2 in AML with inv(8)(p11q13). Cancer Genet Cytogenet 113: 70-72, 1999.
14. Strehl S, Nebral K, König M, Harbott J, Strobl H, Ratei R, Struski S, Bielorai B, Lessard M, Zimmermann M, *et al*: ETV6-NCOA2: A novel fusion gene in acute leukemia associated with coexpression of T-lymphoid and myeloid markers and frequent NOTCH1 mutations. Clin Cancer Res 14: 977-983, 2008.
15. Sumegi J, Streblow R, Frayer RW, Dal Cin P, Rosenberg A, Meloni-Ehrig A and Bridge JA: Recurrent t(2;2) and t(2;8) translocations in rhabdomyosarcoma without the canonical PAX-FOXO1 fuse PAX3 to members of the nuclear receptor transcriptional coactivator family. Genes Chromosomes Cancer 49: 224-236, 2010.
16. Panagopoulos I, Thorsen J, Gorunova L, Micci F and Heim S: Sequential combination of karyotyping and RNA-sequencing in the search for cancer-specific fusion genes. Int J Biochem Cell Biol 53: 462-465, 2014.
17. Wang L, Motoi T, Khanin R, Olshen A, Mertens F, Bridge J, Dal Cin P, Antonescu CR, Singer S, Hameed M, *et al*: Identification of a novel, recurrent HEY1-NCOA2 fusion in mesenchymal chondrosarcoma based on a genome-wide screen of exon-level expression data. Genes Chromosomes Cancer 51: 127-139, 2012.
18. Alaggio R, Zhang L, Sung YS, Huang SC, Chen CL, Bisogno G, Zin A, Agaram NP, LaQuaglia MP, Wexler LH, *et al*: A molecular study of pediatric spindle and sclerosing rhabdomyosarcoma: Identification of novel and recurrent VGLL2-related fusions in infantile cases. Am J Surg Pathol 40: 224-235, 2016.
19. Mosquera JM, Sboner A, Zhang L, Kitabayashi N, Chen CL, Sung YS, Wexler LH, LaQuaglia MP, Edelman M, Sreekantaiah C, *et al*: Recurrent NCOA2 gene rearrangements in congenital/infantile spindle cell rhabdomyosarcoma. Genes Chromosomes Cancer 52: 538-550, 2013.
20. Deguchi K, Ayton PM, Carapeti M, Kutok JL, Snyder CS, Williams IR, Cross NC, Glass CK, Cleary ML and Gilliland DG: MOZ-TIF2-induced acute myeloid leukemia requires the MOZ nucleosome binding motif and TIF2-mediated recruitment of CBP. Cancer Cell 3: 259-271, 2003.
21. Zhuravleva J, Paggetti J, Martin L, Hammann A, Solary E, Bastie JN and Delva L: MOZ/TIF2-induced acute myeloid leukaemia in transgenic fish. Br J Haematol 143: 378-382, 2008.
22. Kaneko Y, Yoshida K, Handa M, Toyoda Y, Nishihira H, Tanaka Y, Sasaki Y, Ishida S, Higashino F and Fujinaga K: Fusion of an ETS-family gene, EIAF, to EWS by t(17;22)(q12;q12) chromosome translocation in an undifferentiated sarcoma of infancy. Genes Chromosomes Cancer 15: 115-121, 1996.
23. Urano F, Umezawa A, Hong W, Kikuchi H and Hata J: A novel chimera gene between EWS and E1A-F, encoding the adenovirus E1A enhancer-binding protein, in extraosseous Ewing's sarcoma. Biochem Biophys Res Commun 219: 608-612, 1996.
24. Braunreiter CL, Hancock JD, Coffin CM, Boucher KM and Lessnick SL: Expression of EWS-ETS fusions in NIH3T3 cells reveals significant differences to Ewing's sarcoma. Cell Cycle 5: 2753-2759, 2006.
25. Tomlins SA, Mehra R, Rhodes DR, Smith LR, Roulston D, Helgeson BE, Cao X, Wei JT, Rubin MA, Shah RB, *et al*: TMPRSS2:ETV4 gene fusions define a third molecular subtype of prostate cancer. Cancer Res 66: 3396-3400, 2006.
26. Han B, Mehra R, Dhanasekaran SM, Yu J, Menon A, Lonigro RJ, Wang X, Gong Y, Wang L, Shankar S, *et al*: A fluorescence in situ hybridization screen for E26 transformation-specific aberrations: Identification of DDX5-ETV4 fusion protein in prostate cancer. Cancer Res 68: 7629-7637, 2008.
27. Hermans KG, Bressers AA, van der Korput HA, Dits NF, Jenster G and Trapman J: Two unique novel prostate-specific and androgen-regulated fusion partners of ETV4 in prostate cancer. Cancer Res 68: 3094-3098, 2008.
28. Liu Y, Yan X and Zhou T: TBCK influences cell proliferation, cell size and mTOR signaling pathway. PLoS One 8: e71349, 2013.
29. Xiong G, Deng L, Zhu J, Rychahou PG and Xu R: Prolyl-4-hydroxylase α subunit 2 promotes breast cancer progression and metastasis by regulating collagen deposition. BMC Cancer 14: 1, 2014.
30. Chang KP, Yu JS, Chien KY, Lee CW, Liang Y, Liao CT, Yen TC, Lee LY, Huang LL, Liu SC, *et al*: Identification of PRDX4 and P4HA2 as metastasis-associated proteins in oral cavity squamous cell carcinoma by comparative tissue proteomics of microdissected specimens using iTRAQ technology. J Proteome Res 10: 4935-4947, 2011.